

EEG-Inception: An Accurate and Robust End-to-End Neural Network for EEG-based Motor Imagery Classification

Ce Zhang¹, Young-Keun Kim², and Azim Eskandarian¹

¹ Mechanical Engineering, Virginia Polytechnic Institute and State University, Blacksburg, VA, USA

² Mechanical and Control Engineering, Handong Global University, Pohang, Gyeongsang, South Korea

E-mail: zce@vt.edu, ykkim@handong.edu, and eskandarian@vt.edu

Abstract

Classification of EEG-based motor imagery (MI) is a crucial non-invasive application in the brain-computer interface (BCI) research. This paper proposes a convolutional neural network (CNN) architecture for accurate and robust EEG-based MI classification that outperforms the state-of-the-art methods. The proposed CNN model, namely EEG-Inception, is built on the backbone of the Inception-Time network, which showed to be highly efficient and accurate for time-series classification. Also, the proposed network is an end-to-end classification, for it takes the raw EEG signals as the input and does not require complex EEG signal-preprocessing. Furthermore, this paper proposes a novel data augmentation method for EEG signals to enhance the accuracy, at least by 3%, and reduce overfitting with limited BCI datasets.

The proposed model outperformed all the state-of-the-art methods by achieving the average accuracy of 88.4% and 88.6% on the 2008 BCI Competition IV 2a (four-classes) and 2b datasets (binary-classes), respectively. Furthermore, it takes less than 0.025 seconds to test a sample, which is suitable for real-time processing. Moreover, the classification standard deviation for nine different subjects achieved the lowest value of 5.5 for the 2b dataset and 7.1 for the 2a dataset, validating that the proposed method is highly robust. From the experiment results, it can be inferred that the EEG-Inception network exhibits a strong potential as a subject-independent classifier for EEG-based MI tasks.

Keywords: Brain-Computer Interface (BCI), Electroencephalography (EEG), Motor Imagery, Neural Network, Time Series Data Augmentation

1. Introduction

Brain-computer interface (BCI) is a direct pathway to communicate between the human brain and external devices [1]. Electroencephalography (EEG) has become one of the most common brain activity recording methods because it is non-invasive and low-cost. An important EEG-based BCI study area is motor imagery (MI), which triggers neural activities by imagining the movement of the body (e.g., left-hand and right-hand movement) [2-4]. Decoding the correct MI neural activities allows patients with motor neuron diseases (e.g., stroke, Parkinson's disease) to rehabilitate partial body movement skills with the assistance of external devices. Besides body rehabilitation, EEG-based MI popular

applications also include wheelchair control [5], robot arm operation [6], and quadcopter manipulation [7].

EEG-based MI signals are non-stationary, where the signal properties such as variance and mean change with time [8]. Furthermore, EEG signals have a low signal-to-noise ratio (SNR) due to numerous artifacts and noises [9]. Decoding the EEG-based MI signals requires advanced signal processing techniques and statistical learning algorithms. Therefore, this paper aims to design an accurate MI classification for non-stationary and subject-dependent EEG signals. The latter addresses the variability in the EEG signals among different subjects (humans). There have been many investigations on the MI tasks classification, conventionally using machine learning algorithms. They are described next in two categories:

1.1 Machine Learning-Based Classification and 1.2 Neural Network-Based Algorithms.

1.1 Machine Learning-based Classification

For classical machine learning algorithms, the EEG signals decoding process includes signal pre-processing, feature extraction, and feature classification. The signal pre-processing objective is to remove noises and artifacts. Common pre-processing methods are independent component analysis (ICA) for ocular artifacts removal, canonical correlation analysis (CCA) for muscle artifacts removal, and bandpass filtering [10-12]. For MI feature extraction, it contains data analysis in time, frequency, and spatial domains. In the time domain, the EEG event-related synchronization and desynchronization (ERD/ERS) features are determined [13]. The frequency-domain analysis is often combined with the time domain through wavelet transforms (WT), or short-time Fourier transforms (STFT) [14-16]. According to Sadiq. M.T.'s work, empirical wavelet transform has also been applied for EEG-based MI classification [17, 18]. In the spatial domain, common spatial pattern (CSP), proposed by G. Pfurtscheller et al., is proved to be effective for EEG-based MI classification [19]. After the CSP algorithm had been developed, K.K. Ang has developed a new CSP-based filter bank (FBCSP) to improve the classification accuracy [20]. Based on the FBCSP, C. Zhang and A. Eskandarian have proposed a computationally efficient CSP algorithm to minimize the computing load [21]. Besides the CSP algorithm, spatial feature dimension reduction has also been proved to be an effective technique. M.T. Sadiq has applied different feature reduction algorithms such as principal component analysis (PCA), and ICA for motor imagery feature extraction [22, 23]. As for feature classification, since the input signals are thoroughly processed, traditional classifiers such as k^{th} nearest neighbor (KNN), linear discriminant analysis (LDA), and support vector machine (SVM) have been proven successful for classification [24-27]. The advantages of classical machine learning algorithms are (i) relatively simple algorithm implementation and (ii) faster training period compared with neural network-based algorithms. However, since the classical machine learning algorithms require manual feature extraction, only limited features can be extracted based on existing algorithms. It is known that the EEG-based MI classification performance heavily relies on feature extraction effectiveness. Therefore, the classical machine learning algorithm EEG-based MI classification results are relatively limited.

1.2 Neural Network-based Algorithms

Recently, researchers have used neural network-based MI classification methods, which have shown better performance than conventional methods. The two popular neural network

structures for EEG-based MI studies are convolutional neural network (CNN) and recurrent neural network (RNN).

The CNN structure can be categorized as one-dimensional CNN (1D-CNN) and multi-dimension CNN (2D/3D-CNN).

The idea of 1D-CNN is to convolve and extract the time series or frequency domain EEG signal features. Y. Li et al. proposed a novel multi-layers 1D-CNN neural network architecture (CP-MixedNet) for MI classification [28]. In their study, forty-four channels of raw EEG signals were employed as input, and multiple 1D-CNN layers were used for spatial, temporal feature extraction. The classification accuracy results indicate that the CP-MixedNet outperforms traditional machine learning algorithms such as FBCSP. However, even though the input EEG signals dimension is reduced from 128 to 44, the computation load can still be decreased by a more intelligent channel selection strategy. Besides convolving the time-series signals, EEG frequency amplitude is also another important input. Y. R. Tabar et al. proposed taking STFT based time-frequency amplitude as input for 1D convolution and a stack auto-encoder architecture for classification [29]. They have compared the CNN combined with the auto-encoder neural network (CNN-SAE) with the CNN architecture and other state-of-the-art algorithms. The results show that the CNN-SAE network average accuracy is around 77.6%, which is better than the 1D-CNN architecture and support vector machine (SVM) classification. However, the proposed auto-encoder classifier has eight layers with the neuron number ranging from 900 to 2, which causes excessive computational load and long training periods. M. Miao et al. have developed a deep 1D-CNN architecture to extract spatial and frequency features for MI feature extraction [30]. According to their comparison, their proposed model is around 10% higher than the CSP-based feature extraction methods.

Since each 1D-CNN layer can only convolve and extract EEG features in one dimension (time, frequency, or spatial), some researchers apply 2D/3D-CNN to extract features from multiple dimensions the same time. For EEG-based MI studies, most multi-dimension CNN structure ideas are borrowed from object detection algorithms such as AlexNet [31]. B.H. Lee et al. proposed an end-to-end CNN for multiclass MI classification [32]. Part of their proposed ERA-CNN model is inspired by the hierarchical deep CNN that is developed for visual recognition. The ERA-CNN implements multiple 2D-CNN with kernel matrix size ranges from 36 to 288. The proposed neural network achieves around 66% for seven-class MI classification. Inspired by visual recognition, some researchers have converted the EEG time series classification (TSC) problem to an image classification problem. T. Yang et al. have proposed a convolutional neural network model with a multiple dimensional kernel matrix [33]. They have converted the EEG signals into an image as

input and compared the 2D and 3D kernel matrix feature extraction and classification performance. According to the experiment results, the 2D kernel matrix generally exhibits higher accuracy than the 3D kernel matrix.

For the RNN model, long-short term memory (LSTM), inspired by natural language processing, is one of the most popular structures for EEG-based MI classification. Since raw EEG signals are in time series, the time domain's correlation can be used for MI class prediction. P. Wang et al. have employed the LSTM to achieve robust classification on EEG-based MI [34]. In the proposed LSTM model, the input signals are normalized raw EEG data. After one-dimensional aggregate approximation and channel selection, the EEG signals are fed into the LSTM model. The proposed algorithm number of parameters is only 746, and the average classification accuracy for Group I dataset is 76.47%. Even though the classification accuracy is not the best compared with other state-of-art algorithms, the small size of model parameters shows that the computational load is much lower than other neural networks. Besides directly feeding time-series EEG signal to the LSTM model, J. Jeong et al. designed a CNN and LSTM combination model for MI decoding and a robotic arm control [35]. The EEG signals feature are extracted through a pre-trained CNN, then the extracted features are predicted by LSTM networks. Based on their two experiments, the robotic arm moving towards correct directions success rates are 0.6 and 0.43, respectively.

The abovementioned related works indicated that CNN based classification methods for EEG MI had achieved higher accuracy than conventional methods. However, there are several issues that require more extensive research to improve the classification. The first issue is enhancing the classification accuracy. Most neural network-based classification methods have accuracy ranges from high 70% to low 80%. The second issue is the availability of EEG datasets. Since the EEG-based MI experiments on human subjects are complex processes, the available dataset size is too small. The last issue is developing a subject-independent model. Currently, EEG-based MI classifiers are subject-dependent due to variations of neuronal feedbacks among different subjects. It is necessary to develop subject-independent MI models to be readily applied to new subjects without acquisitions of training datasets.

Therefore, this paper proposes a new CNN network to increase the accuracy of MI-EEG signal classification and robustness to subject-dependency. The proposed network is called EEG-Inception and uses several inceptions [36] and residual [37, 38] modules as the backbone. Also, to tackle the limitation in the training data, a new data augmentation of EEG signals is proposed, which could increase the average accuracy by 3%.

The contributions of the EEG-Inception model can be categorized as:

- A CNN-based classification achieving 88.6% in the average accuracy outperforming all other state-of-the-art methods for binary classes dataset and 88.4% for four classes dataset.
- A novel data augmentation method for EEG signal to reduce overfitting and further improve classification accuracy with small training data size.
- A High robustness subject-dependent dataset with a low standard deviation in classifying different subjects
- High potential for a subject-independent EEG-based MI classification.

The rest of the paper is organized as follows. Section II illustrates the EEG-Inception neural network and the novel EEG data augmentation method. Section III describes the experimental protocol of the open-source dataset that we used for evaluation. Section IV presents the proposed EEG-Inception model performance and the data augmentation effectiveness results. In section V, we conclude the proposed algorithm results and propose potential new future works based on the EEG-Inception neural network.

2. Proposed Network Architecture

This section introduces the architecture of the proposed EEG-Inception model and the data augmentation method, as illustrated in Figure 1.

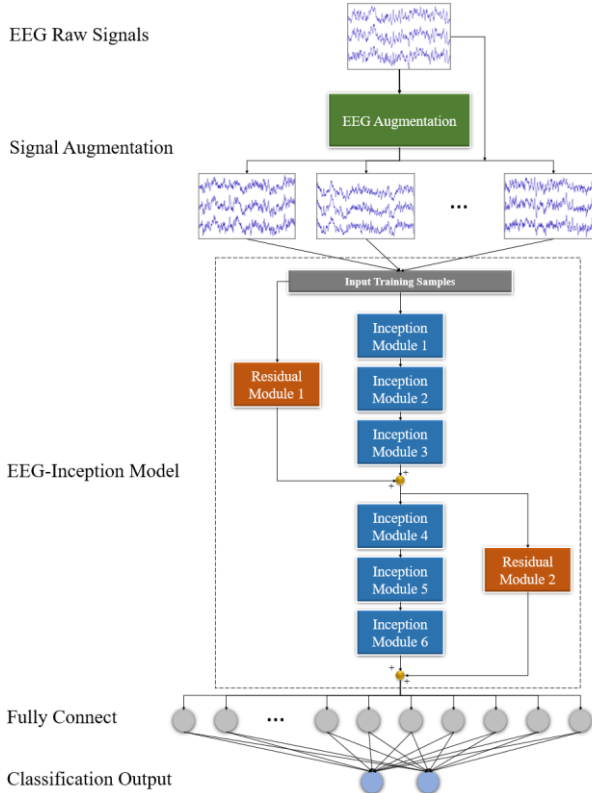


Figure 1. Proposed Algorithm Overall Scheme. The proposed algorithm contains a novel data augmentation method, an EEG-Inception model, and classification.

2.1. EEG-Inception Neural Network

The backbone of the proposed EEG-Inception network is an ensemble of multiple inception modules and residual modules, as shown in Figure 1. The Inception module is inspired by image classification as it not only extracts deep features but also maintains a low computational load. The residual module is often used to diminish the "vanishing gradient problem" caused by deeper layers and activation functions.

The proposed network is composed of the six Inception module and two residual modules, as illustrated in Figure 1. Details about the inception and residual module functions are illustrated below.

2.1.1 Inception Module

The inception module can be categorized as an "initial inception module" and "intermediate inception module." Both modules contain a bottleneck layer, multiple convolutional layers, and a pooling layer (Figure 2a and 2b). The difference between the "initial" and the "intermediate inception module" is the bottleneck layer depth. For the "initial inception module," the bottleneck layer increases the data depth from the number of EEG input channels to N while, for the

"intermediate inception module," the bottleneck layer decreases the data depth from $[4 \times N]$ to N . In an EEG-based deep learning study, the collected EEG channels are commonly considered as the depth of the input data. For our dataset, the number of EEG channels is three for the binary classes dataset and twenty-two for the four classes dataset. Therefore, to extract deeper features from low data depth, the "initial inception module" bottleneck layer increases the input signal depth dimension with a N depth, one length, and one width kernel matrix. For the other inception modules in our proposed neural network, the bottleneck layer reduces the data depth from $[4 \times N]$ to N to lower the computational load.

For the pooling layer, the max-pooling with the kernel size of three is selected. The objective of the max-pooling layer is to reduce the dimension of the output. After the pooling layer, a 1D convolutional layer with a 1×1 kernel matrix is applied to enlarge the depth of the data dimension to increase the number of learning parameters.

For the convolution layers, several 1D convolutions have been conducted with different kernel sizes. For the binary classes dataset, we employed three 1D convolutional layers with kernel sizes of 25×1 , 75×1 , and 125×1 , respectively, as shown in Figure 2a. For the four-classes dataset, we use five 1D convolutional layers with the kernel size of 25×1 , 75×1 , 125×1 , 175×1 , and 225×1 , respectively, as shown in Figure 2b. The large kernel size can significantly diminish the data size and convolve the EEG signal with one millisecond, three milliseconds, and five milliseconds, etc. By employing different kernel sizes, more features can be extracted and concatenated together for classification.

The batch normalization layer is a standard normalization algorithm that preventing overfitting and decreasing training steps [39].

At the end of an inception module, a ReLU activation function is employed to preserve the features of the positive values. Compared with the traditional sigmoid and the "tanh" () activation function, the ReLU function overcomes the "vanishing gradient problem," allowing the model to gain higher accuracy.

2.1.2 Residual Module

According to Figure 1, the residual module is applied after every three inception modules. The residual module is a convolutional layer with a kernel size of 1×1 , and the equation is

$$y = \mathcal{F}(x_0, \{W_i\}) + x \quad (1)$$

where x_0 is the input vector, $\mathcal{F}(x_0, \{W_i\})$ represents the residual mapping from the input vector, x is the output layer from the inception module, and y is the summation between

the residual layer output and the inception module output. K. He et. al. proves that the residual learning framework can effectively solve the learning degradation problem caused by deeper layers [34]. Thus, in our EEG-Inception module, we implement a residual module for every three inception modules to prevent learning degradation.

In summary, the proposed EEG-Inception neural network contains six inception modules and two residual modules, as shown in Figure 1.

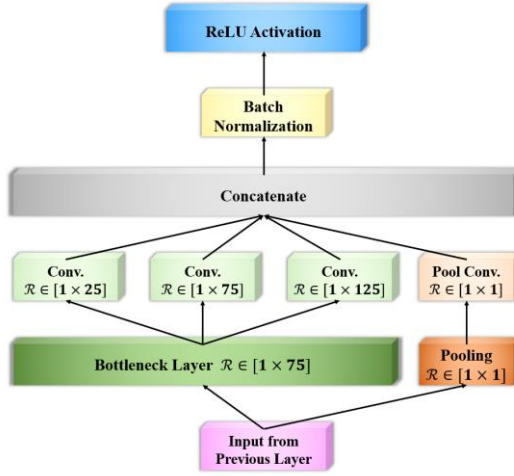


Figure 2a. Proposed EEG-Inception Neural Network Overall Architecture for the Binary-Classes Dataset. The EEG-Inception model contains a bottleneck layer and three convolutional layers.

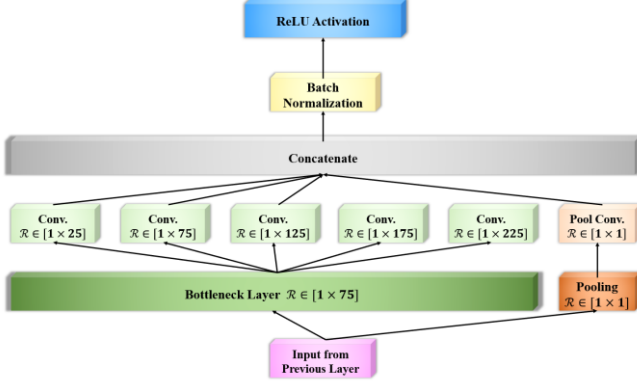


Figure 2b. Proposed EEG-Inception Neural Network Overall Architecture for the Four-Classes Dataset. The EEG-Inception model contains a bottleneck layer and five convolutional layers.

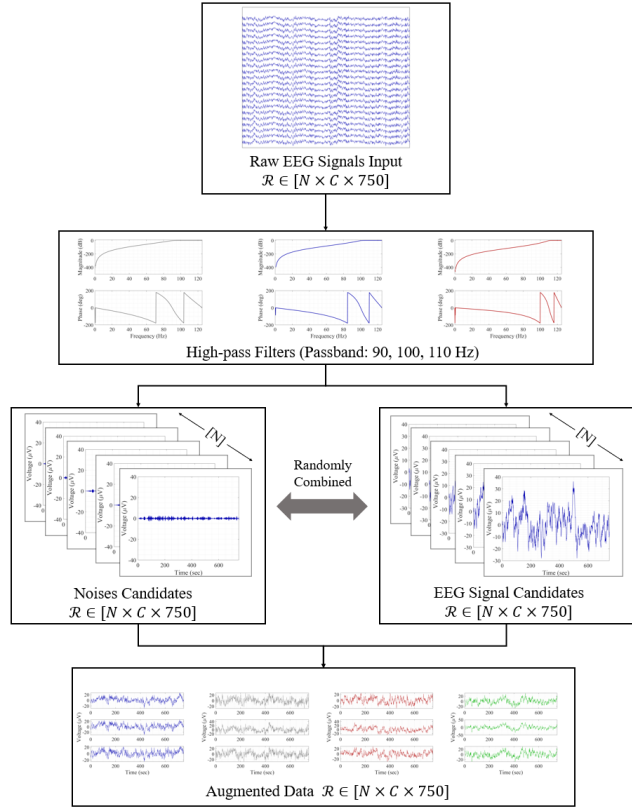


Figure 3. Data Augmentation Scheme. The extracted noise candidates are combined randomly with the signal candidates.

2.2 Data Augmentation

The objective of data augmentation is to minimize the overfitting issue by transforming the training data to extend the data size. EEG-based motor imagery data size is usually small due to the lengthy and challenging experiment [40]. Thus, it is necessary to conduct data augmentation processing for EEG motor imagery classification. Unlike standard computer vision data augmentation, EEG signals are non-stationary, which cannot be rotated, stretched, or scaled because these methods change the time-series signals properties. Therefore, noise addition is one of the best methods to expand the data size [41]. According to S. Muthukumaraswamy's work, most brain activities exist in a frequency range from 0-100 Hz, and the frequency above 100 Hz can be considered as artifacts and noises [42]. Thus, our proposed data augmentation method is to extract the above-100 Hz signal from one trial, then apply it to another trial, presented in Figure 3.

According to Figure 3, we have designed an 8th order Butterworth high-pass filter with a cut-off frequency of 100 Hz to extract the noise candidates at first. Then, use the original EEG signals to subtract their noise candidates. Finally, adding noise candidates extracted from another trial, as shown in Equation 2

$$S_{aug}(i) = S_0(i) - S_n(i) + S_n(k) \quad (2)$$

where $S_{aug}(i)$ is the augmented signal for the i^{th} trial, $S_0(i)$ is the i^{th} trial original signal, S_n is the noise candidates, and k represents a random trial number. This process is repeated three times. Thus, the training data size is four times larger than the original training size. The augmented signal comparison with the original signal is shown in Figures 4 and 5.

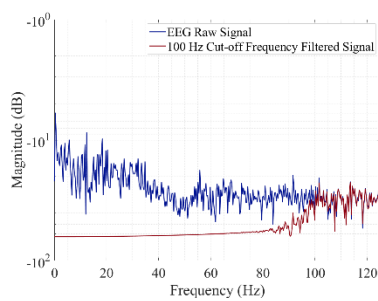


Figure 4a. Frequency Domain of Raw Signal and Extracted Noises. The extracted noise candidate is at a cut-off frequency of 100 Hz.

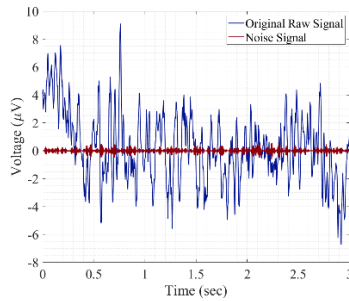


Figure 4b. Time Domain of Raw Signal and Extracted Noises

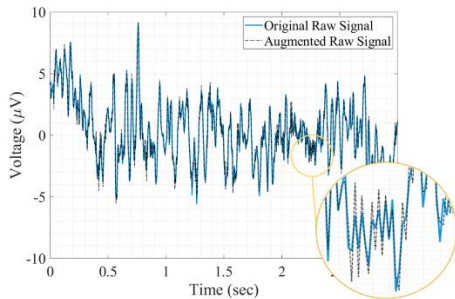


Figure 5a. Original and Augmented Signal for Subject 1 Trial 1

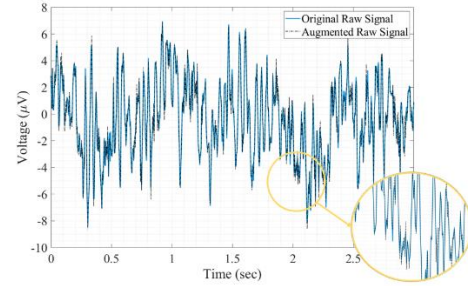


Figure 5b. Original and Augmented Signal for Subject 4 Trial 4

2.3 Ablation Study on Layer Depth

An ablation study, commonly applied in neuroscience research, is employed for artificial neural network performance analysis [43]. The objective is to investigate the classification accuracy change with different numbers of neural network layers or different features. In this study, we have tested our neural network by varying the depth of the convolutional kernel matrix. The convolutional kernel matrix dimension has varied from six to sixty-four for the binary-classes dataset and twenty-four to eighty-four for the four-classes dataset. According to our assumption, the computation time should increase because of the increasing convolutional kernel matrices depth, while the classification accuracy trend is unpredictable.

3. Dataset and Experiment Protocol

3.1 Dataset Description

To compare the performance with other state-of-the-art algorithms, we have used two publicly available datasets from the BCI Competition IV, namely dataset 2a and dataset 2b [44]. Both datasets contain EEG and EOG signals with a sampling frequency of 250 Hz from nine subjects. For dataset 2a, subjects were required to perform four classes (left hand, right hand, feet, and tongue) MI, and for dataset 2b, subjects were asked to perform binary classes MI tasks (left hand and right hand). Figure 6 presents the localizations of the EEG channels for both datasets 2a and 2b. Twenty-two channels are provided by the dataset 2a, and three channels are provided by the dataset 2b.

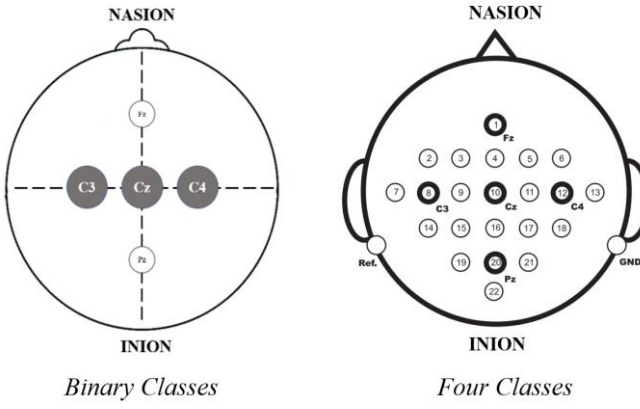


Figure 6. Dataset 2a and 2b Channels Localization. The 2a dataset contains 22 channels while the 2b dataset contains three channels

For the binary-classes dataset, each subject has conducted five sessions where the first two sessions are MI without results feedback (MI w/o feedback), and the last three sessions are MI with results feedback (MI w/ feedback). Figure 7 shows the paradigm of the MI w/o feedback for one trial. During the MI w/o session, the subjects are asked to perform 60 trials of MI tasks per-class, 120 trials in total. At each trial, the motor imagery period is 3 seconds. The scheme for the MI w/ feedback session of one trial is shown in Figure 8. In the MI w/ feedback session, the subjects are asked to perform 80 trials of motor imagery tasks per-class, 160 trials in total. At each trial, the motor imagery period is around 4 seconds. Moreover, the MI w/ feedback session evaluates the motor imagery performance for every trial where the green smiley face represents a correct motor imagery task while the sad red face indicates a wrong task.



Figure 7. MI Binary Class w/o Feedback Session Paradigm for One Trial

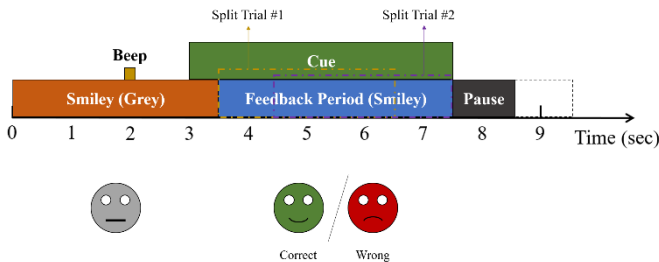


Figure 8. MI Binary Class w/ Feedback Session Paradigm for One Trial.

For the four classes dataset, each subject has conducted two sessions without results feedback. The experiment procedures

are similar to the two classes dataset, as shown in Figure 9. The four classes dataset contains 72 trials per class (288 trials in total). At each trial, the motor imagery period is 3 seconds.

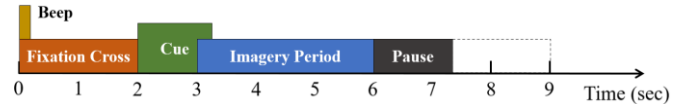


Figure 9. MI Four Classes Session Paradigm for One Trial

3.2 Experiment Protocol

Since both dataset 2a and 2b sizes are too small for neural network model training and evaluation, some modifications on the input signal are necessary. For dataset 2b, we doubled the number of trials in the last three sessions by selecting the first three-second imagery period as one trial, and the last three-second imagery period is as another trial shown in Figure 8. Thus, by combining all sessions, the total number of motor imagery trials is 1200 for every subject, and the length of each trial is 3 seconds, which are used as input signals. For dataset 2a, since the motor imagery period is three seconds fixed, we only applied more augmented signals for training.

To ensure the input training data correctness, rejected trials labeled by the dataset are removed. Therefore, the total number of trials is varied based on different subjects. In the dataset, we set the training and testing data ratio around 3:1, and the details about the training and testing samples for every subject are presented in Table 1.

Table 1. Training/Testing Samples Summary for All Subjects at Both Binary Class and Four Classes Dataset

	Acceptance Rate (%)	Train w/o Augmentation	Train w/ Augmentation	Test
		Binary Classes Dataset		
S1	75.33%	678	2034	226
S2	79.17%	712	2136	238
S3	72.83%	655	1965	219
S4	97.17%	874	2622	292
S5	89.25%	803	2409	268
S6	77.58%	698	2094	233
S7	79.83%	718	2154	240
S8	74.50%	670	2010	224
S9	78.50%	706	2118	236
Four Classes Dataset				
S1	86.46%	498	2988	140
S2	86.28%	497	2982	139
S3	84.27%	488	2928	137
S4	76.56%	441	2646	123
S5	84.03%	484	2904	135
S6	67.71%	390	2340	110
S7	86.46%	498	2988	138
S8	83.51%	481	2886	135
S9	78.13%	450	2700	127

4. Results and Discussions

The EEG-Inception model is evaluated through an open-source dataset 2a and 2b from the BCI competition IV. The

proposed algorithm testing results are presented from five aspects: (1) the proposed model training process, (2) the ablation study outcome, (3) the data augmentation method effectiveness, (4) the proposed algorithm accuracy comparison with other state-of-art algorithms, and (5) a preliminary examination of the proposed EEG-Inception model for subject-independent study.

4.1 Training Process

The EEG-Inception neural network model is written with Python programming language-based Pytorch platform [45]. To achieve faster computation speed, the model is trained by an Nvidia GeForce RTX 2080Ti graphics card. During the training process, a backpropagation method is employed for the neural network weight update. Since the input signals are non-stationary, and the model is relatively complex, we use adaptive moment estimation (Adam) as the optimizer with a general learning rate of 0.005. The Adam equation is shown in equation 3

$$\theta_{t+1} = \theta_t - \frac{\eta}{\sqrt{\hat{v}_t + \epsilon}} \hat{m}_t \quad (3)$$

where θ is the updated parameters, m_t and v_t are the first and second-moment gradient, respectively, η is the general learning rate, and ϵ is a smoothing term. The loss is calculated by the binary class cross-entropy loss function

$$H_p(q) = -\frac{1}{N} \sum_{i=1}^N y_i \cdot \log(p(y_i)) + (1 - y_i) \cdot \log(1 - p(y_i)) \quad (4)$$

where y is the label, $p(y)$ is the predicted label probability, and N is the total sample size. In our experiment, the training iteration is 100 to ensure the model is converged, and the batch size is set to be 32 for less calculation memory.

4.2 Ablation Study

As stated before, our ablation study is conducted by varying the convolution kernel matrix depth. Table 2 summarizes the number of model parameters and model size with different kernel matrix depths for binary-classes model and four-classes model. When increasing the layer depth, both model parameters and the model size are linearly increasing. Figure 10 presents the model classification accuracies and computation time results with varied kernel matrix depths for dataset 2b. Similar behavior can also be observed on the dataset 2a results. With increasing kernel matrix depths, the computation time follows an exponentially increasing trend while the classification accuracy is unpredictable. The classification accuracy is not guaranteed to improve by simply increasing kernel matrix depth because a deeper kernel matrix causes the model overfitting. Based on this result, the final convolution kernel matrix depth is twelve for dataset 2b and forty-eight for dataset 2a. The total model parameters are over twenty thousand for the binary classes model and over eight

million for the four classes model, and the total model sizes for binary-classes and four-classes models are 10.83 and 34.10 megabytes, respectively. To better understand the proposed Inception-EEG model, the binary-classes Inception EEG model summary are tabulated in Table 3.

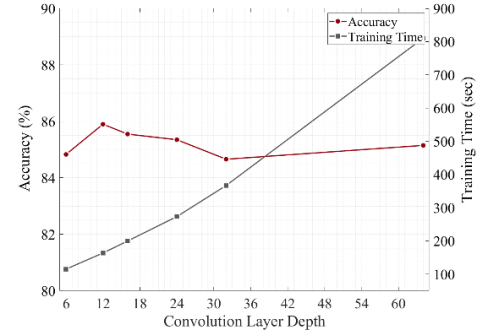


Figure 10. Training Time and Classification Accuracy with Different Convolution Layer Depth

Table 2. Model Parameters and Size Comparison with Different Layer Depth

Layer Depth	Binary Classes Dataset		Four Classes Dataset		
	Total Parameters	Total Size (MB)	Layer Depth	Total Parameters	Total Size (MB)
6	51,386	5.23	24	2,236,468	8.60
12	204,002	10.83	36	5,021,356	19.20
16	361,986	14.77	48	8,917,348	34.10
24	812,930	23.18	60	13,924,444	53.20
32	1,443,842	32.27	72	20,042,664	76.50
64	5,767,170	75.49	84	27,271,948	104.00

Table 3. EEG-Inception Neural Network Architecture Summary for Binary Classes Dataset and Four Classes Dataset

Layer	Output Shape	Param #
Initial Inception Module	[48, 750]	32,628
Intermediate Inception Module_1	[48, 750]	33,708
Intermediate Inception Module_2	[48, 750]	33,708
Residual Module_1	[48, 750]	288
Intermediate Inception Module_3	[48, 750]	33,708
Intermediate Inception Module_4	[48, 750]	33,708
Intermediate Inception Module_5	[48, 750]	33,708
Residual Module_2	[48, 750]	2,448
Average Pooling	[48, 750]	-
Linear	[1, 2]	98
Initial Inception Module		
MaxPooling-1d	[3, 750]	-
Convolution-1d	[12, 750]	48
Convolution-1d	[12, 750]	48
Convolution-1d	[12, 750]	3,612
Convolution-1d	[12, 750]	10,812
Convolution-1d	[12, 750]	18,012
BatchNormalization-1d	[48, 750]	96
ReLU Activation	[48, 750]	-
Intermediate Inception Module		
MaxPooling-1d	[3, 750]	-
Convolution-1d	[12, 750]	48
Convolution-1d	[12, 750]	48
Convolution-1d	[12, 750]	3,612
Convolution-1d	[12, 750]	10,812
Convolution-1d	[12, 750]	18,012
BatchNormalization-1d	[48, 750]	96
ReLU Activation	[48, 750]	-
Residual Module_1		
Convolution-1d	[48, 750]	192
BatchNormalization-1d	[48, 750]	96
ReLU Activation	[48, 750]	-
Residual Module_2		
Convolution-1d	[48, 750]	2,352
BatchNormalization-1d	[48, 750]	96
ReLU Activation	[48, 750]	-
Parameters Summary		
Total Parameters	204,002	
Trainable Parameters	204,002	

4.3 Effect of Data Augmentation

The effectiveness of the proposed data augmentation method can be evaluated from the accuracy convergence speed and the classification accuracy improvement.

For accuracy convergence speed, the proposed data augmentation method is faster than the dataset without augmentation. As shown in Figure 11, the classification accuracy with the data augmentation method is converged after 10-20 iterations while the without augmentation method is not converged until 40-60 iterations. Since the proposed data augmentation method randomly combined the noise candidates with the signal candidates, the randomness of the training samples is improved, but the signal temporal pattern features and frequency domain features are still well preserved. Thus, with increasing the randomness of the training samples and the dataset size, the convergence speed is faster than the training without using the proposed augmentation method.

For classification results, the overall accuracy for the proposed data augmentation method is 3-4% higher than the without data augmentation training for both datasets. According to Table 4, the data augmentation method average accuracy is 2.8% higher for the binary-classes dataset and 3.6% higher for the four-classes dataset. By observing the binary-classes dataset S2-S5, and the four-classes dataset S1, S5, and S6, we find that the proposed data augmentation method can significantly improve the classification accuracy

when the original accuracy is low. It is known that the main reason for low classification accuracy is artifacts caused by ocular, muscle, and other miscellaneous situations. For the "poor-performed" subjects, the noises artifacts are usually more inconsistent than the "well performed" subjects. Therefore, the proposed data augmentation method effectively extracts certain noise artifacts and randomly combined them with the MI signals, which increases the number of noisy MI samples for better model learning and higher testing classification accuracy.

Table 4. Classification Accuracy Comparison with Augmentation and non-Augmentation

	Binary Classes Dataset		Four Classes Dataset	
	InceptionTime w/ Aug.	InceptionTime w/o Aug.	InceptionTime w/ Aug.	InceptionTime w/o Aug.
S1	87.20%	84.51%	89.61%	81.52%
S2	79.79%	77.31%	80.01%	78.68%
S3	84.19%	77.17%	96.17%	94.09%
S4	96.32%	95.21%	81.26%	80.48%
S5	94.06%	93.66%	83.76%	79.66%
S6	89.27%	88.19%	81.20%	76.98%
S7	82.98%	81.90%	94.75%	91.47%
S8	90.63%	89.45%	98.28%	91.36%
S9	92.80%	84.55%	90.50%	89.17%
Average	88.58%	85.77%	88.39%	84.82%
Std. dev.	5.50	6.46	7.06	6.59

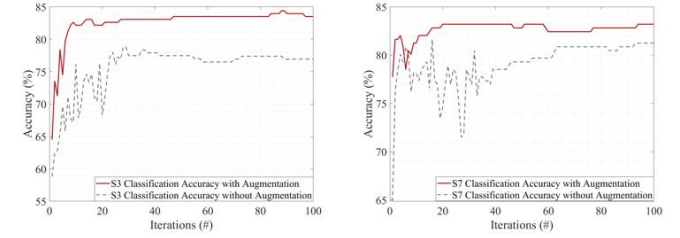


Figure 11a. Selected Subjects Binary-Classes Dataset Classification Accuracy Curve Comparison

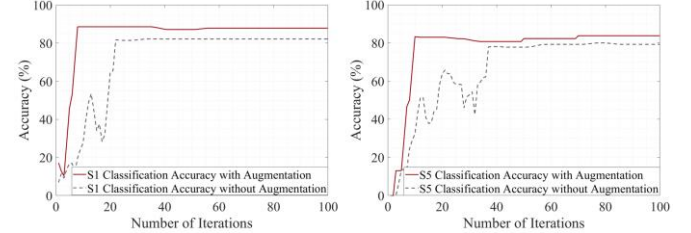


Figure 11b. Selected Subjects Four-Classes Dataset Classification Accuracy Curve Comparison

4.4 Comparison with State-of-the-Art Algorithms

We have compared our EEG-Inception neural network with six popular EEG-based binary motor imagery classification algorithms [46-51] for both the binary-classes dataset and four-classes dataset. To ensure a fair comparison, all the algorithms use the BCI Competition IV 2b and 2a dataset, and the results are shown in Table 5 and 6, respectively. For both datasets, we evaluate the proposed EEG-Inception network

through classification accuracy, computation time, and the standard deviation of classification accuracy among all subjects. In the remaining of this section, binary-classes dataset results are discussed at first, and the four-classes dataset results are illustrated then.

4.4.1 Binary-Classes Dataset Results

As for average classification accuracies, the proposed EEG-Inception neural network is the highest among all state-of-art algorithms for the binary-classes dataset, which is 1% higher than the HS-CNN and almost 10% higher than the FBCSP algorithm. For single-subject classification accuracy examination, the EEG-Inception model exhibits better classification accuracies for "poorly performed" subjects. Figure 12 shows the EEG-Inception model accuracy comparison results with the top three state-of-art algorithms. According to this figure, #2 and #3 subjects exhibit the worst classification accuracies for all algorithms. The proposed EEG-Inception model maintains the classification accuracy by around 80%, which is approximately 12.5% higher than the other state-of-art algorithms. The leading causes of #2 and #3 low classification accuracies are unclear neuronal features and artifact contamination. Therefore, based on the #2 and #3 classification results, the proposed EEG-Inception algorithm can extract more effective features when subject brain signals are covered by noises and artifacts.

The computation time for the EEG-Inception network is 0.0187s for one sample. Instead of adding convolutional layers in series, the EEG-Inception network applies several convolutional layers in parallel to extract MI features from different time lengths. Therefore, the EEG-Inception network is more computationally efficient compared with other deep convolutional neural networks.

Besides the classification accuracy and computation time, we compare the average standard deviation (std. dev.) among all subjects. The proposed EEG-Inception neural network std. dev. is 5.5, which is 35.14% less than the HS-CNN algorithm and 58.31% less than the average std. dev. among all state-of-art algorithms. Such low std. dev. of the proposed algorithm indicates that the proposed algorithm is robust to all subjects, which has the potential for subject-independent learning.

4.4.2 Four-Classes Dataset Results

The EEG-Inception network classification accuracy for the four-classes dataset is 88.39%, which ranked 2nd among all other state-of-art algorithms [48, 50, 52-55]. The only algorithm that surpasses the EEG-Inception network for multiclass classification is the HS-CNN algorithm. The main reason that EEG-Inception is lower than the HS-CNN algorithm is because of the small training data size. Compared with the binary-classes dataset, the original four-classes

dataset training sample is around 35% smaller. The EEG-Inception applies five parallel convolutional kernel matrices, which requires a more extensive training dataset to learn the kernel matrices parameters for better feature extraction performance. With the improvement of the EEG-based MI experiment protocol, creating a larger EEG-based MI dataset is feasible. Therefore, we believe that the EEG-Inception network is more suitable for larger dataset training, and the classification accuracy can be further improved.

As for computation time, the EEG-inception takes 0.0215s for testing one sample. The reason for the longer computation time than the binary-classes dataset is because the four-classes dataset contains 22 EEG channels, and the number of parallel convolutional matrices is increased from 3 to 5. Thus, the computation time is increased. However, this computation time is still fast enough for real-time processing.

The EEG-Inception network std. dev. among all subjects is 7.06 (Table 6). Similar to the classification accuracy results, the std. dev. for EEG-Inception network can be further decreased with a larger dataset. However, such low std. dev. still shows that EEG-Inception is robust to all subjects and has the potential for subject-independent learning.

Table 5. Binary Classes Dataset Classification Accuracy Comparison with State-of-Art Methods

	WT-Isomap [46]	Boltzman Machine [47]	EMD-MI [48]	RSMM [49]	HS-CNN [50]	Bi-spectrum [51]	EEG-Inception
S1	84.60	81.00	62.80	72.50	80.50	77.00	87.20
S2	66.30	65.00	67.10	56.40	70.60	64.50	79.79
S3	62.90	66.00	98.70	55.60	85.60	61.00	84.19
S4	95.80	98.00	88.40	97.20	94.60	96.50	96.32
S5	89.20	93.00	96.30	88.40	98.30	82.00	94.06
S6	97.90	88.00	75.30	78.70	86.60	84.50	89.27
S7	82.10	82.00	72.20	77.50	89.60	75.00	82.98
S8	86.30	94.00	87.80	91.90	95.60	91.00	90.63
S9	97.10	91.00	85.30	83.40	87.40	87.00	92.80
Average	84.69	84.22	81.54	77.96	87.64	79.83	88.58
Std. Dev.	12.72	11.94	12.74	14.57	8.48	11.73	5.50

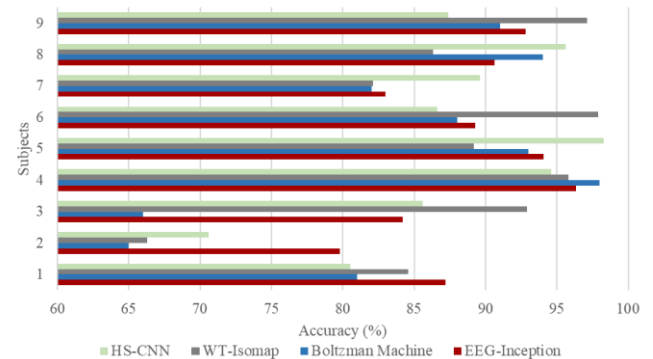


Figure 12. Binary Class Classification Accuracy Comparison with the Top Three State-of-Art Algorithms

Table 6. Four Classes Dataset Classification Accuray Comparison with State-of-Art Methods

	DFFS [52]	EMD-MI [48]	MEMD-Rieman [53]	Adaptive-MI [54]	R-CSP [55]	HS-CNN [50]	EEG-Inception
s1	63.69	66.7	91.49	90.28	88.89	90.07	89.61
s2	61.97	63.9	60.56	54.17	51.39	80.28	80.01
s3	91.09	77.8	94.16	93.75	96.53	97.08	96.17
s4	61.72	63.2	76.72	64.58	70.14	89.66	81.26
s5	63.41	72.2	58.52	57.64	54.86	97.04	83.76
s6	66.11	70.1	68.52	65.28	71.53	87.04	81.2
s7	59.57	64.6	78.57	65.2	81.25	92.14	94.75
s8	62.84	76.4	97.01	90.97	93.75	98.51	98.28
s9	84.46	77.1	93.85	85.42	93.75	82.31	90.5
Average	68.32	70.2	79.93	73.84	78.01	91.57	88.39
Std. Dev.	11.29	5.92	14.99	15.72	17.01	6.49	7.06

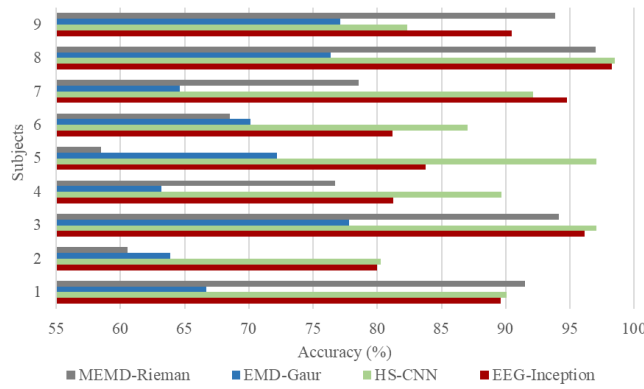


Figure 13. Four Classes Classification Accuracy Comparison with the Top Three State-of-Art Algorithms

4.5 Preliminary Subject-Independent Classification Examination

Since the EEG-Inception neural network std. dev. is the smallest compared with other state-of-art algorithms, it has the potential to be used for subject-independent classification. These results are preliminary because the EEG-Inception subject-dependent model is directly applied without further fine-tuning and adjustment. Figure 14, and Table 7 and 8 present the ROC curve and confusion matrices for the subject-independent classification for both datasets, respectively.

For the binary-classes dataset, the classification accuracy is 77.5%, which is 12.5% lower than the EEG-Inception subject dependent model but close to the RSMM and Bi-spectrum algorithms. Furthermore, according to the ROC curve, we find that the proposed data augmentation method is still effective in the subject-independent study where the AUC result is 0.03 higher than the w/o augmentation method.

For the four-classes dataset, the classification accuracy is 65.88%, which is 22% lower than the EEG-Inception subject-dependent model. Since the SoftMax equation ranges from 0 to 1, it is acceptable to see classification accuracy drop when the number of target classes increased from two to four due to the smaller probability range boundary for each class. Furthermore, the dataset size for the four-classes dataset is not large enough for subject-independent classification. Thus, the four-classes dataset subject-independent classification accuracy is lower than the binary-classes dataset subject-independent results. However, 65.88% still shows the strong potential that the EEG-Inception network can be applied for subject-independent classification with further modification.

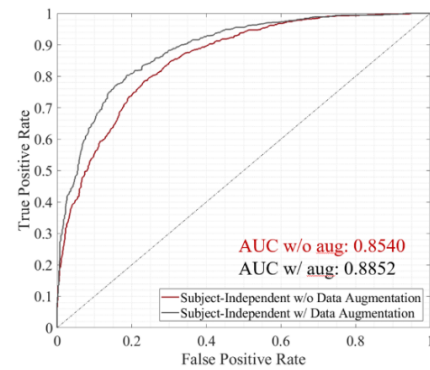


Figure 14. ROC Curve for Subject-Independent at Binary Classes Classification

TABLE 7. Confusion Matrix for Binary Classes Subject-Independent Classification

		Binary Classes Dataset Subject Independent Classification		Accuracy
		Predicted	Actual	
Actual	Left	998	406	71.08%
	Right	85	687	88.99%
Avg. Accuracy	77.44%		Kappa	0.55
F1-score	0.737		Recall	0.628

TABLE 8. Confusion Matrix for Four Classes Subject-Independent Classification

		Four Classes Dataset Subject Independent Classification				Accuracy
		Predict	Actual	Left	Right	
	Left	253	32	3	5	86.35%
	Right	60	214	6	12	73.29%
	Foot	79	57	159	16	51.13%
	Tongue	74	51	11	152	52.78%
Avg. Accuracy		65.88%		Kappa	0.544	
F1-score		0.655		Recall	0.657	

5. Conclusions and Future Works

In this paper, we presented a novel data augmentation method and modified the Inception Time neural network for EEG-based motor imagery, namely EEG-Inception. The data augmentation method can diminish the overfitting issue caused by the small data size. The proposed EEG-Inception neural network achieves an accuracy of 88.58% for the binary-classes dataset and 88.39 for the four-classes dataset.

Moreover, the std. dev among all subjects is 5.5 and 7.1 for the binary-classes dataset and four-classes dataset, respectively. The low std. dev. represents the proposed algorithm features extraction is robust among all subjects. We have also conducted a preliminary examination for subject-independent analysis, and the classification accuracy is 77.5% and 65.9% for binary-classes and four-classes, respectively.

In the future, we will further investigate the specificity and generality of each layer from the EEG-Inception neural network. After finding the specificity and generality of the EEG-Inception network, we are going to fine-tune the EEG-Inception model so that it fits for the EEG-based MI subject independent classification task.

References

[1] Krucoff MO, Rahimpour S, Slutzky MW, Edgerton VR, Turner DA. Enhancing Nervous System Recovery through Neurobiologics, Neural Interface Training, and Neurorehabilitation. *Front. Neurosci.* 2016;10:584.

[2] Pfurtscheller G, Aranibar A. Event-related cortical desynchronization detected by power measurements of scalp EEG. *Electroencephalography and Clinical Neurophysiology*. 1977;42(6):817-26.

[3] Pfurtscheller G, Brunner C, Schlogl A, Lopes da Silva FH. Mu rhythm (de)synchronization and EEG single-trial classification of different motor imagery tasks. *NeuroImage*. 2006;31(1):153-9.

[4] Padfield N, Zabalza J, Zhao H, Masero V, Ren J. EEG-Based Brain-Computer Interfaces Using Motor-Imagery: Techniques and Challenges. *Sensors (Basel)*. 2019;19(6):1423.

[5] Yu Y, Zhou Z, Liu Y, Jiang J, Yin E, Zhang N, Wang Z, Liu Y, Wu X, Hu D. Self-Paced Operation of a Wheelchair Based on a Hybrid Brain-Computer Interface Combining Motor Imagery and P300 Potential. *IEEE Transactions on Neural Systems and Rehabilitation Engineering*. 2017;25(12):2516-26.

[6] Rakshit A, Konar A, Nagar AK. A hybrid brain-computer interface for closed-loop position control of a robot arm. *IEEE/CAA Journal of Automatica Sinica*. 2020;7(5):1344-60.

[7] Khan MJ, Zafar A, Hong K, editors. Hybrid EEG-NIRS based active command generation for quadcopter movement control. 2016 International Automatic Control Conference (CACS); 2016 9-11 Nov. 2016.

[8] Zhao H, Zheng Q, Ma K, Li H, Zheng Y. Deep Representation-Based Domain Adaptation for Nonstationary EEG Classification. *IEEE Transactions on Neural Networks and Learning Systems*. 2020;1-11.

[9] Haumann NT, Parkkonen L, Kliuchko M, Vuust P, Brattico E. Comparing the Performance of Popular MEG/EEG Artifact Correction Methods in an Evoked-Response Study. *Computational Intelligence and Neuroscience*. 2016;2016:7489108.

[10] Zhang C, Eskandarian A. A Survey and Tutorial of EEG-Based Brain Monitoring for Driver State Analysis. *IEEE/CAA Journal of Automatica Sinica*. 2020

[11] Akhtar MT, Mitsuhashi W, James CJ. Employing spatially constrained ICA and wavelet denoising, for automatic removal of artifacts from multichannel EEG data. *Signal Processing*. 2012;92(2):401-16.

[12] Clercq WD, Vergult A, Vanrumste B, Paesschen WV, Huffel SV. Canonical Correlation Analysis Applied to Remove Muscle Artifacts From the Electroencephalogram. *IEEE Transactions on Biomedical Engineering*. 2006;53(12):2583-7.

[13] Neuper C, Müller-Putz GR, Scherer R, Pfurtscheller G. Motor imagery and EEG-based control of spelling devices and neuroprostheses. In: Neuper C, Klimesch W, eds. *Progress in Brain Research*. vol 159; Elsevier; 2006. p. 393-409.

[14] Yang H, Guan C, Chua KS, Chok SS, Wang CC, Soon PK, Tang CK, Ang KK. Detection of motor imagery of swallow EEG signals based on the dual-tree complex wavelet transform and adaptive model selection. *J Neural Eng*. 2014;11(3):035016.

[15] Hsu W-Y, Sun Y-N. EEG-based motor imagery analysis using weighted wavelet transform features. *Journal of Neuroscience Methods*. 2009;176(2):310-8.

[16] Bashar SK, Bhuiyan MIH. Classification of motor imagery movements using multivariate empirical mode decomposition and short time Fourier transform based hybrid method. *Engineering Science and Technology, an International Journal*. 2016;19(3):1457-64.

[17] Sadiq MT, Yu X, Yuan Z, Aziz MZ. Motor imagery BCI classification based on novel two-dimensional modelling in empirical wavelet transform. *Electronics Letters [Internet]*. 2020; 56(25):[1367-9 pp.].

[18] Sadiq MT, Yu X, Yuan Z, Fan Z, Rehman AU, Li G, Xiao G. Motor Imagery EEG Signals Classification Based on Mode Amplitude and Frequency Components Using Empirical Wavelet Transform. *IEEE Access*. 2019;7:127678-92.

[19] Pfurtscheller G, Guger C, Ramoser H, editors. *EEG-based brain-computer interface using subject-specific spatial filters*. *Engineering Applications of Bio-Inspired Artificial Neural Networks*; 1999 1999//; Berlin, Heidelberg: Springer Berlin Heidelberg.

[20] Kai Keng A, Zheng Yang C, Haihong Z, Cuntai G, editors. *Filter Bank Common Spatial Pattern (FBCSP) in Brain-Computer Interface*. 2008 IEEE International Joint Conference on Neural Networks (IEEE World Congress on Computational Intelligence); 2008 1-8 June 2008.

[21] Zhang C, Eskandarian A, editors. *A Computationally Efficient Multiclass Time-Frequency Common Spatial Pattern Analysis on EEG Motor Imagery*. 2020 42nd Annual International Conference of the IEEE Engineering in Medicine & Biology Society (EMBC); 2020 20-24 July 2020.

[22] Sadiq MT, Yu X, Yuan Z. Exploiting dimensionality reduction and neural network techniques for the development of expert brain-computer interfaces. *Expert Syst. Appl.* 2021;164:114031.

[23] Sadiq MT, Yu X, Yuan Z, Zeming F, Rehman AU, Ullah I, Li G, Xiao G. Motor Imagery EEG Signals Decoding by Multivariate Empirical Wavelet Transform-Based Framework for Robust Brain-Computer Interfaces. *IEEE Access*. 2019;7:171431-51.

[24] Shang-Lin W, Chun-Wei W, Pal NR, Chih-Yu C, Shi-An C, Chin-Teng L, editors. *Common spatial pattern and linear discriminant analysis for motor imagery classification*. 2013 IEEE Symposium on Computational Intelligence, Cognitive Algorithms, Mind, and Brain (CCMB); 2013 16-19 April 2013.

[25] Ma Y, Ding X, She Q, Luo Z, Potter T, Zhang Y. Classification of Motor Imagery EEG Signals with Support Vector Machines and Particle Swarm Optimization. *Comput Math Methods Med*. 2016;2016:4941235.

[26] Chatterjee R, Bandyopadhyay T, editors. *EEG Based Motor Imagery Classification Using SVM and MLP*. 2016 2nd International Conference on Computational Intelligence and Networks (CINE); 2016 11-11 Jan. 2016.

[27] Bhaduri S, Khasnobish A, Bose R, Tibarewala DN, editors. *Classification of lower limb motor imagery using K Nearest Neighbor and Naïve-Bayesian classifier*. 2016 3rd International

Conference on Recent Advances in Information Technology (RAIT); 2016 3-5 March 2016.

[28]Li Y, Zhang X, Zhang B, Lei M, Cui W, Guo Y. A Channel-Projection Mixed-Scale Convolutional Neural Network for Motor Imagery EEG Decoding. *IEEE Transactions on Neural Systems and Rehabilitation Engineering*. 2019;27(6):1170-80.

[29]Tabar YR, Halici U. A novel deep learning approach for classification of EEG motor imagery signals. *Journal of Neural Engineering* [Article]. 2017;14(1):11.

[30]Miao M, Hu W, Yin H, Zhang K. Spatial-Frequency Feature Learning and Classification of Motor Imagery EEG Based on Deep Convolution Neural Network. *Comput Math Methods Med*. 2020;2020:1981728-.

[31]Krizhevsky A, Sutskever I, Hinton GE. ImageNet classification with deep convolutional neural networks. Proceedings of the 25th International Conference on Neural Information Processing Systems - Volume 1; Lake Tahoe, Nevada: Curran Associates Inc.; 2012. p. 1097–105.

[32]Lee B, Jeong J, Shim K, Lee S, editors. Classification of High-Dimensional Motor Imagery Tasks Based on An End-To-End Role Assigned Convolutional Neural Network. ICASSP 2020 - 2020 IEEE International Conference on Acoustics, Speech and Signal Processing (ICASSP); 2020 4-8 May 2020.

[33]Yang T, Phua KS, Yu J, Selvaratnam T, Toh V, Ng WH, Ang KK, So RQ, editors. Image-based Motor Imagery EEG Classification using Convolutional Neural Network. 2019 IEEE EMBS International Conference on Biomedical & Health Informatics (BHI); 2019 19-22 May 2019.

[34]Wang P, Jiang A, Liu X, Shang J, Zhang L. LSTM-Based EEG Classification in Motor Imagery Tasks. *IEEE Transactions on Neural Systems and Rehabilitation Engineering*. 2018;26(11):2086-95.

[35]Jeong J, Shim K, Kim D, Lee S. Brain-Controlled Robotic Arm System Based on Multi-Directional CNN-BiLSTM Network Using EEG Signals. *IEEE Transactions on Neural Systems and Rehabilitation Engineering*. 2020;28(5):1226-38.

[36]Fawaz HI, Lucas B, Forestier G, Pelletier C, Schmidt D, Weber J, Webb GI, Idoumghar L, Muller P-A, Petitjean F. InceptionTime: Finding AlexNet for Time Series Classification. *ArXiv*. 2019;abs/1909.04939.

[37]He K, Zhang X, Ren S, Sun J, editors. Deep Residual Learning for Image Recognition. 2016 IEEE Conference on Computer Vision and Pattern Recognition (CVPR); 2016 27-30 June 2016.

[38]Szegedy C, Liu W, Jia Y, Sermanet P, Reed S, Anguelov D, Erhan D, Vanhoucke V, Rabinovich A. Going deeper with convolutions. *2015 IEEE Conference on Computer Vision and Pattern Recognition (CVPR)*. 2015:1-9.

[39]Ioffe S, Szegedy C. Batch Normalization: Accelerating Deep Network Training by Reducing Internal Covariate Shift. *ArXiv*. 2015;abs/1502.03167.

[40]Lotte F, Bougrain L, Cichocki A, Clerc M, Congedo M, Rakotomamonjy A, Yger F. A review of classification algorithms for EEG-based brain-computer interfaces: a 10 year update. *Journal of Neural Engineering*. 2018;15(3):031005.

[41]Wang F, Zhong S-h, Peng J, Jiang J, Liu Y, editors. Data Augmentation for EEG-Based Emotion Recognition with Deep Convolutional Neural Networks. MultiMedia Modeling; 2018 2018//; Cham: Springer International Publishing.

[42]Muthukumaraswamy SD. High-frequency brain activity and muscle artifacts in MEG/EEG: a review and recommendations. *Frontiers in human neuroscience*. 2013;7:138-.

[43]Meyers R, Lu M, Puiseau CWd, Meisen T. Ablation Studies in Artificial Neural Networks. *ArXiv*. 2019;abs/1901.08644.

[44]Tangermann M, Müller K-R, Aertsen A, Birbaumer N, Braun C, Brunner C, Leeb R, Mehring C, Miller K, Mueller-Putz G, et al. Review of the BCI Competition IV. *Front. Neurosci.* [Review]. 2012;6(55).

[45]Paszke A, Gross S, Massa F, Lerer A, Bradbury J, Chanan G, Killeen T, Lin Z, Gimelshein N, Antiga L, et al. PyTorch: An Imperative Style, High-Performance Deep Learning Library. *ArXiv*. 2019;abs/1912.01703.

[46]Li M-A, Zhu W, Liu H-n, Yang J-F. Adaptive Feature Extraction of Motor Imagery EEG with Optimal Wavelet Packets and SE-Isomap. *Applied Sciences*. 2017;7:390.

[47]Lu N, Li T, Ren X, Miao H. A Deep Learning Scheme for Motor Imagery Classification based on Restricted Boltzmann Machines. *IEEE Transactions on Neural Systems and Rehabilitation Engineering*. 2017;25(6):566-76.

[48]Gaur P, Pachori RB, Hui W, Prasad G, editors. An empirical mode decomposition based filtering method for classification of motor-imagery EEG signals for enhancing brain-computer interface. 2015 International Joint Conference on Neural Networks (IJCNN); 2015 12-17 July 2015.

[49]Zheng Q, Zhu F, Heng P. Robust Support Matrix Machine for Single Trial EEG Classification. *IEEE Transactions on Neural Systems and Rehabilitation Engineering*. 2018;26(3):551-62.

[50]Dai G, Zhou J, Huang J, Wang N. HS-CNN: a CNN with hybrid convolution scale for EEG motor imagery classification. *Journal of Neural Engineering*. 2020;17(1):016025.

[51]Shahid S, Prasad G. Bispectrum-based feature extraction technique for devising a practical brain-computer interface. *J Neural Eng*. 2011;8(2):025014.

[52]Luo J, Feng Z, Zhang J, Lu N. Dynamic frequency feature selection based approach for classification of motor imageries. *Computers in Biology and Medicine*. 2016;75:45-53.

[53]Gaur P, Pachori RB, Wang H, Prasad G. A multi-class EEG-based BCI classification using multivariate empirical mode decomposition based filtering and Riemannian geometry. *Expert Syst. Appl.* 2018;95:201-11.

[54]Raza H, Cecotti H, Li Y, Prasad G. Adaptive learning with covariate shift-detection for motor imagery-based brain-computer interface. *Soft Computing*. 2016;20(8):3085-96.

[55]Lotte F, Guan C. Regularizing Common Spatial Patterns to Improve BCI Designs: Unified Theory and New Algorithms. *IEEE Transactions on Biomedical Engineering*. 2011;58(2):355-62.